MODELING THERMAL RESPONSE OF POLYMER COMPOSITE HYDROGEN CYLINDERS SUBJECTED TO EXTERNAL FIRES

Saldi, Z. and Wen, J.X.*
Warwick FIRE, School of Engineering, University of Warwick, Coventry CV4 7AL, United Kingdom

***Contact: jennifer.wen@warwick.ac.uk**

ABSTRACT

With the anticipated introduction of hydrogen fuel cell vehicles to the market, there is an increasing need to address the fire resistance of hydrogen cylinders for onboard storage. Sufficient fire resistance is essential to ensure safe evacuation in the event of car fire accidents. The authors have developed a Finite Element (FE) model for predicting the thermal response of composite hydrogen cylinders within the frame of the open source FE code Elmer. The model accounts for the decomposition of the polymer matrix and effects of volatile gas transport in the composite. Model comparison with experimental data has been conducted using a classical one-dimensional test case of polymer composite subjected to fire. The validated model was then used to analyze a type-4 hydrogen cylinder subjected to an engulfing external propane fire, mimicking a published cylinder fire experiment. The external flame is modelled and simulated using the open source code FireFOAM. A simplified failure criteria based on internal pressure increase is subsequently used to determine the cylinder fire resistance.

1.0 INTRODUCTION

In the pursuit of zero carbon emission from power generation, hydrogen has been recognized as a promising energy carrier and is being increasingly used in a variety of applications. One of the prominent examples of hydrogen utilization is in fuel cells for automotive power generation. Hydrogen fuel cell vehicles (HFCV) are currently being developed by a number of car manufacturers. They are expected to be commercialized in the near future.

The commercialisation of HFCVs requires onboard storage of hydrogen at sufficient quantity to cover reasonable driving distances. While different storage techniques are under development, the only commercially available technology stores compressed hydrogen at 35-70 MPa in a cylinder tank typically made of Carbon-Fibre-Reinforced Polymer (CFRP). One of the important aspects in the design of cylinder tanks is their fire resistance. In the probable event of HFCV fire accidents, the tank must be strong enough to withstand the thermomechanical loading arising from an external fire. According to the regulation, the tank must also be equipped with Temperature-activated Pressured Release Device (TPRD), which will vent the hydrogen from the tank whenever a peculiarly high temperature corresponding to the fire is detected. A sufficient tank fire resistance would mean that the venting of hydrogen can proceed slowly, such that there will be no overpressure in the case of no ignition, or if a flame does ignite, it will not be harmful to the surrounding people or objects in terms of length and heat radiation [1]. Unfortunately, the fire resistance of current generations of hydrogen tanks is only around 12 minutes for type 3 cylinders (with aluminum liner) [2], and 3.5-6.5 minutes for type 4 cylinders (with plastic liner) [3]. Such fire resistance is still unacceptable to allow for a timely evacuation by fire brigades or first responders. For comparison, venting of 35 MPa hydrogen gas through a 5 mm TPRD orifice within 3 minutes corresponds with a flow rate of about 390 g/s that causes an overpressure of 10-20 kPa within 2 seconds [4]. This is high enough to destroy a residential garage. Under the same venting condition at 70 MPa in an open space, the safety distance would be about 50 m, which is intolerable to the public. Accordingly, enhanced fire resistance of onboard hydrogen cylinder tanks is urgently needed.

A number of previous studies have attempted to address the characteristics of polymer composite and/or CFRP material subjected to external fires, both for general purpose and onboard hydrogen storage applications. The use of computational modelling and simulation is commonplace in these studies. The thermal response of polymer composite for general application has been extensively modelled [5-9], taking into account a number of important physical and chemical aspects, such as thermal decomposition reaction of the CFRP, the transport of volatile gas towards the heated surface, pressure rise in the CFRP, and thermal expansion/contraction. For onboard hydrogen storage application, numerical models have been employed to study the hydrogen cylinder behaviour subjected to both engulfing fire [10,11] and localized fire [12-14].

Of the above numerical studies on thermal response of hydrogen storage cylinders, none has incorporated the prediction of cylinder fire resistance into the coupled model of external fire and cylinder thermal field simulations. Coupling of fire simulation and cylinder simulation has actually been reported [10,13,14], but the model did not predict the fire resistance. Moreover, the cylinder thermal model only considered pure conductive heat transfer, without effects of resin decomposition and volatile gas transport.

In this paper, thermal response prediction of a type-4 CFRP hydrogen cylinder subjected to engulfing external propane fires, mimicking a published hydrogen tank fire exposure burst experiment [3], is presented. The initial internal pressure is 34.3 MPa. The simulation of the cylinder thermal field is carried out using the open source Finite Element (FE) code Elmer [15], taking into account the CFRP resin decomposition and volatile gas transport. The thermal loading from the external flame is represented as heat flux predicted in a separate simulation of propane pool fire using CFD code FireFOAM [16]. The predicted thermal response, in conjunction with a simplified failure criteria, is subsequently analyzed in order to determine the fire resistance of the cylinder.

2.0 NUMERICAL MODELS

The numerical simulations in this paper employ two mathematical models. The first model is a Finite Element model to simulate the thermal response of the hydrogen cylinder, and the second model is a Finite Volume CFD model for predicting external fire impinging on the cylinder wall. At this stage, several assumptions and simplifications are made. The fire loading on the cylinder is represented by a constant heat flux based on the predicted mean heat flux obtained from CFD simulation.

2.1 Finite Element Model for Hydrogen Cylinder Thermal Response

The thermal process in the heating of CFRP cylinder by external fire is initially dominated by heat transfer in the form of heat conduction. After the temperature reaches a certain threshold, decomposition reaction starts to take place. At the onset of decomposition, heat may be absorbed or released from the reacting CFRP resin and fibers. As the heating proceeds, the composite degrades to form gaseous products, which are convectively transported away towards the heated surface. The corresponding thermal model thus incorporates these three important ingredients, i.e. heat conduction, decomposition, and volatile gas convection. The governing equation in the model is expressed as follows:

$$\rho C_p\left(\frac{\partial T}{\partial t}\right) - \nabla\cdot\left(k\nabla T\right) = -\dot{m}_g C_{p,g}\frac{\partial T}{\partial x} + \frac{\partial \rho}{\partial t}\left(Q_{dec} + h_c - h_g\right) \quad (1)$$

In the above equation, r is the CFRP density, C_p CFRP specific heat, T temperature, k thermal conductivity, $\dot{m}_g$ the gas mass flux, $C_{p,g}$ the specific heat of volatile gas, Q_{dec} the heat of

decomposition, h_c the composite enthalpy, and h_g the gas enthalpy. The gas mass flux in the first source term on the right hand side of the above equation can be formulated as:

$$\dot{m}_g = \int_l^x \frac{\partial \rho}{\partial t} dx \tag{2}$$

The parameter $\frac{\partial r}{\partial t}$, the time rate of change of decomposition, is generally expressed as an n[th]-order kinetic rate equation of Arrhenius form, as follows:

$$\frac{\partial r}{\partial t} = -A r \left(\frac{m - m_f}{m_0} \right)^n \exp\left(\frac{E_a}{RT} \right) \tag{3}$$

where A is the pre-exponential factor, m mass, m_0 initial mass, m_f final mass, E_a activation energy, and R gas constant.

The composite enthalpy is formulated as:

$$h_c = \int_{T_0}^{T} C_p \, dT \tag{4}$$

and the gas enthalpy is expressed as:

$$h_g = \int_{T_0}^{T} C_{p,g} \, dT \tag{5}$$

2.2 CFD Model for External Fire Simulation

A Finite-Volume-based CFD model is used to simulate the external propane fire. The model [17] employs the extended Eddy Dissipation Concept (EDC) combustion model within the frame of Large Eddy Simulation (LES) to deal with turbulence [18, 19]. This model has been developed and implemented in the dedicated fire simulation solver FireFOAM, within the open source CFD code OpenFOAM.

3.0 VALIDATION OF FE MODEL FOR THERMAL RESPONSE PREDICTION

The Finite Element model for thermal response prediction has been implemented in the open source code Elmer. The model has been validated using a test problem of Haveg H41N polymer composite material heated on one side [5], which undergoes thermal decomposition during the heating. The material thickness is 3 cm. The comparison of time evolution of temperature at four locations in the through-thickness direction of the material between Elmer simulation results and experiments is shown in Figure 1. The monitored location x = 0.1 cm is the closest to the heated side, therefore it is associated with the highest temperature rise. The model results are in fairly good agreement with experimental results, thus demonstrating its potential capability of simulating the hydrogen cylinder problem studied in this paper.

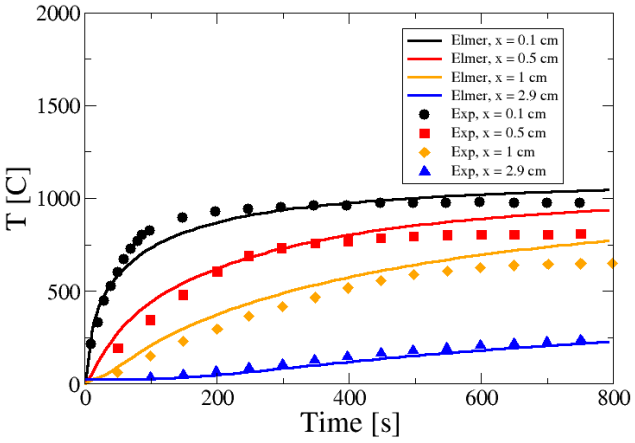

Figure 1. Comparison of time evolution of temperature at four locations in through-thickness direction between Elmer simulation and experiment [5].

4.0 SIMULATION PARAMETERS

4.1 3-D Fire LES Computation

In this study, for the external fire simulation the same conditions used in a published hydrogen tank fire exposure burst experiment [3] are reproduced, in which a propane fire engulfed a Type-4 hydrogen cylinder. The corresponding 3-D computational domain/setup for the LES using FireFOAM is shown in Figure 2. The cylinder is mounted above the ground, where an array of fuel nozzles is installed. The cylinder axis is oriented parallel to the ground. The nozzle configuration (number, arrangement, and diameter of the nozzles and distance between the cylinder wall and the nozzle) is unknown from the paper [3], and thus based on the setup photograph in the paper, these parameters are estimated and given in Table 1. The approximate heat release rate in the experiment is 370 kW (assuming a 95% burning efficiency), corresponding to a propane flow rate of 580 scfh (8.26 gr/s).

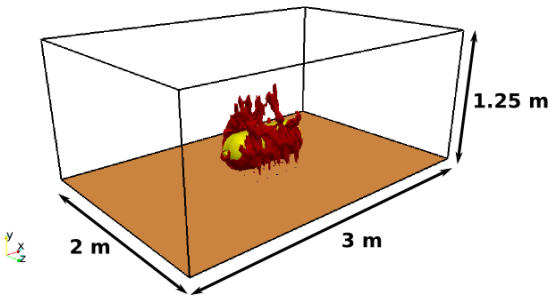

Figure 2. 3-D computational domain.

The computational domain is divided into 1,369,988 grid cells, occupying a multi-block space. The meshes were built using expansion of the cell size from the nozzle to the side outlet boundaries, from the bottom to top outlet boundary, and from the cylinder wall to the other boundaries, with expansion ratio of 1.2-1.4. The minimum cell size in the x-z plane is 2.5 mm, associated with the cells at the fuel nozzle, whereas the maximum cell size is 0.2 m, located adjacent to the side outlet boundaries. In the vertical direction, the minimum cell size is 1 mm, corresponding to the cells right above the nozzle

and bottom boundaries, whereas the maximum cell size is 0.1 m, located right below the top outlet boundary. The thickness of the cells at the cylinder wall is 2.26 mm.

The LES employs a subgrid scale turbulence model based on one-equation eddy model, in which the subgrid turbulent kinetic energy is solved. Radiation is modelled by solving the radiative heat transfer equation using the finite volume discrete ordinates model (fvDOM). The spatial discretization of the convective terms in the governing equations is based on the Gauss limited linear scheme, which satisfies the Total Variation Diminishing (TVD) characteristics. The gradient and diffusive terms are discretized using the central difference scheme with 2^{nd}-order accuracy. The unsteady terms are treated using the 1^{st}-order implicit Euler scheme, with a typical time step of 10^{-5}-10^{-4} second and maximum Courant number of 0.8. The PIMPLE algorithm is chosen to deal with the pressure-velocity coupling.

Table 1. Propane nozzle configuration

Parameters	Values
Distance between cylinder wall and nozzles [m]	0.25
Number of nozzle (total, in x-, in z-direction)	15, 5, 3
Distance between nozzles in x-direction [cm]	11.5
Distance between nozzles in z-direction [cm]	18.4
Nozzle diameter [cm]	1.0
Flow rate [kg/s]	0.00826

4.2 Cylinder Tank Geometry and Material Properties

The hydrogen cylinder tank is 909 mm long with an outer diameter of 325 mm. The 2-D axisymmetric geometry of the cylinder tank is shown in Figure 3, in which only a half of the tank is simulated in order to save computational time. Accordingly, symmetric boundary conditions are imposed on the tank axis. The total thickness of the CFRP and the plastic liner is 32 mm (27 mm and 5 mm, respectively). The material properties of the tank (CFRP and plastic liner) are given in Table 2. The type of the plastic liner is high-density polyethylene (HDPE) and the metallic body is aluminium.

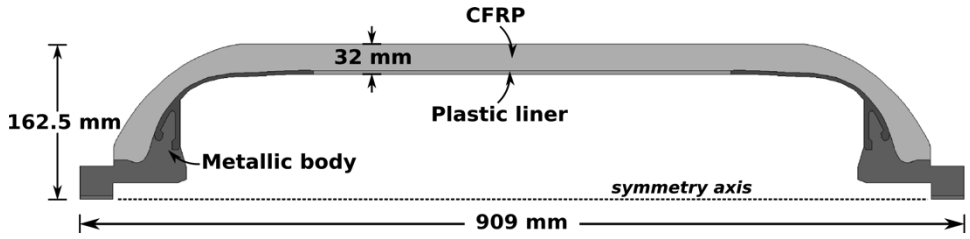

Figure 3. Cylinder tank geometry.

4.3 Coupling of CFD and FE Models and Boundary Conditions

At this stage, for simplicity a one-way coupling between the CFD and FE models is employed. From the 3-D CFD fire simulation, the mean heat flux distribution on the cylinder wall is obtained at quasi-steady state, which accounts for both mean convective and radiative heat transfers from the flame to the cylinder. From the 3-D mean heat flux distribution, the circumferential slice with the maximum mean heat flux is determined, and the mean heat flux distribution along the cylinder wall in that slice is used as the boundary condition for the subsequent 2-D axisymmetric FE simulation to predict the cylinder thermal response. Additionally, radiative heat loss on the cylinder wall is also taken into account, using surface emissivity of 0.5. At the internal wall, the heat exchange rate between the hydrogen gas and the plastic liner is represented by a heat transfer coefficient of 1000 $W/m^2/K$ [12].

Table 2. Material properties.

Properties	Values	Refs.
CFRP		
Initial density [kg/m^3]	1750	[13]
Heat conductivity [W/m^2/K]	6.5	[13]
Specific heat capacity [J/kg/K]	-19+3T	[13]
Pre-exponential factor [1/s]	500.0	[12]
Order of reaction [-]	0	[12]
Activation energy [kJ/kg/mole]	6.05 x 10^4	[12]
Specific heat of gas [J/kg/K]	2386.5	[12]
Heat of decomposition [J/kg]	3.5 x 10^5	[12]
HDPE liner		
Density [kg/m^3]	960	[20]
Heat conductivity [W/m^2/K]	0.45	[20]
Specific heat capacity [J/kg/K]	2250	[20]
Aluminium boss		
Density [kg/m^3]	2700	[13]
Heat conductivity [W/m^2/K]	218	[13]
Specific heat capacity [J/kg/K]	902	[13]

5.0 RESULTS AND DISCUSSION

5.1 Fire Simulation

The development of fire at t = 0.2, 0.5, 1.0, 1.2, 1.5, and 1.8 s is shown in Figure 4, in which the instantaneous temperature iso-contour of 1100 K is used. It has to be emphasized that 1100 K is not the temperature of flame. The iso-contour of 1100 K is used in Figure 4 simply for a better visualization. The regions occupying higher temperatures are of smaller volumes. In the flame simulation, the maximum temperature is only around 1600 K, which is around 600 K lower than the adiabatic flame temperature of propane (~2200 K). This significant drop may be caused by two factors: (i) Very high radiative heat loss from the flame to the tank and surrounding (total radiant fraction is 0.35-0.4); and (ii) The currently used CFD-FE coupling is only one-way, i.e. heat flux from the flame is imposed on the boundary of the FE model and no heat transfer from the tank CFD domain is fed back to the flame CFD domain whatsoever.

As the fire develops, it engulfs mostly the lower part of the cylinder, followed by the lateral sides. At the top part of the cylinder, the fire mostly affects the lateral sides too, whereas the top center surface and the top surface of the domes are only marginally affected by the fire, as indicated by the low local heat flux. This can be shown in more details in Figure 5, where the cylinder wall heat flux distribution is given. The maximum heat flux is around 100 kW/m^2, and in a large part of the cylinder surface, the heat flux is around 50 kW/m^2. This is similar to the order of magnitude expected and typical for a fire scenario.

The LES of the fire development for the configuration studied in this paper is a computationally demanding simulation, and at this stage the time scale of 6.5 minutes, i.e. the failure time of the type-4 cylinder in the cylinder fire experiment [3], is beyond the capability of our available computing resources. Accordingly, an assumption that at t = 1.8 s, the fire has reached a quasi-steady state is used. This assumption can be supported by the more or less constant height of the isotherm in the 1.0-1.8 s interval with some degree of intermittency, as shown in Figure 4. Furthermore, the instantaneous and mean temperature are also monitored at two locations close to the cylinder surface, i.e. point 1 and 2, with (x,y,z) coordinates of (-0.3, -0.17, 0.0) m and (0.3, -0.17, 0.0) m, respectively, as shown in

Figure 6. It is clearly shown that the instantaneous temperature has reached a quasi-steady state at t = 1.8 s.

5.2 Hydrogen Cylinder Thermal Response

Using the LES computation, the mean heat flux at the cylinder wall at quasi-steady state (t = 1.8 s) can be obtained, as given in Figure 7 (left). For the simulation of the thermal response of the cylinder, three circumferential slices based on the orientation angle in the y-z plane (θ) are selected. This is done in order to afford the 2-D axisymmetric simulation (with a sketch in Figure 3), instead of a full 3-D simulation of the thermal field, aimed at saving computational time. The axial distribution of the mean heat flux at $\theta = 90^0$, 180^0, 270^0 is shown in Figure 7 (right). The top surface at the mid-plane of the cylinder ($\theta = 0^0$) is omitted, since at this angle the cylinder wall is only marginally affected by the fire such that the mean heat flux is much lower than the rest of the surface. The orientation angles $\theta = 90^0$ and 270^0 correspond to two symmetrical lateral sides of the cylinder, whereas the angle $\theta = 180^0$ corresponds to the lower surface at the mid-plane of the cylinder. As the symmetry of the mean heat flux between $\theta = 90^0$ and 270^0 is preserved, the present analysis only includes the thermal response for $\theta = 90^0$ and 180^0. The mean heat flux distribution at these angles is used as boundary conditions in the cylinder thermal simulation using Elmer.

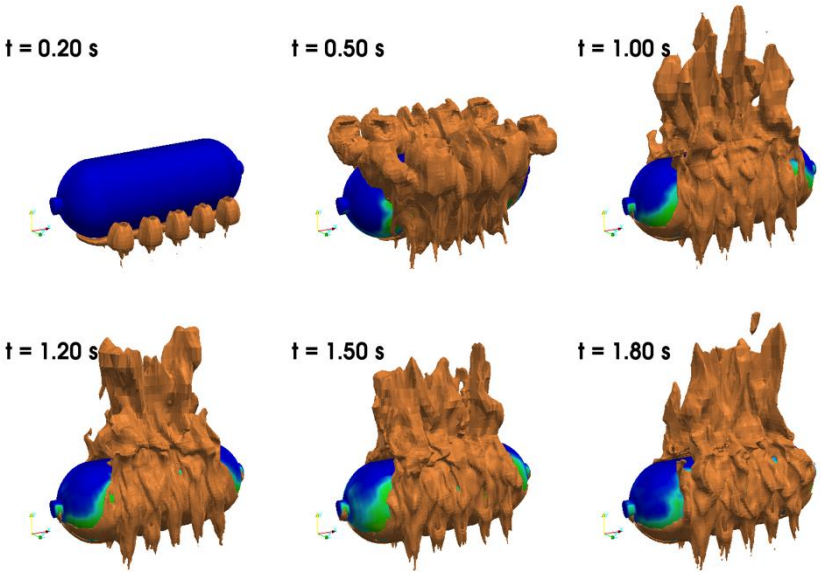

Figure 4. Development of fire, represented by temperature iso-contour of 1100 K, at t = 0.2, 0.5, 1.0, 1.2, 1.5, and 1.8 s. The colour on the cylinder corresponds to the local heat flux.

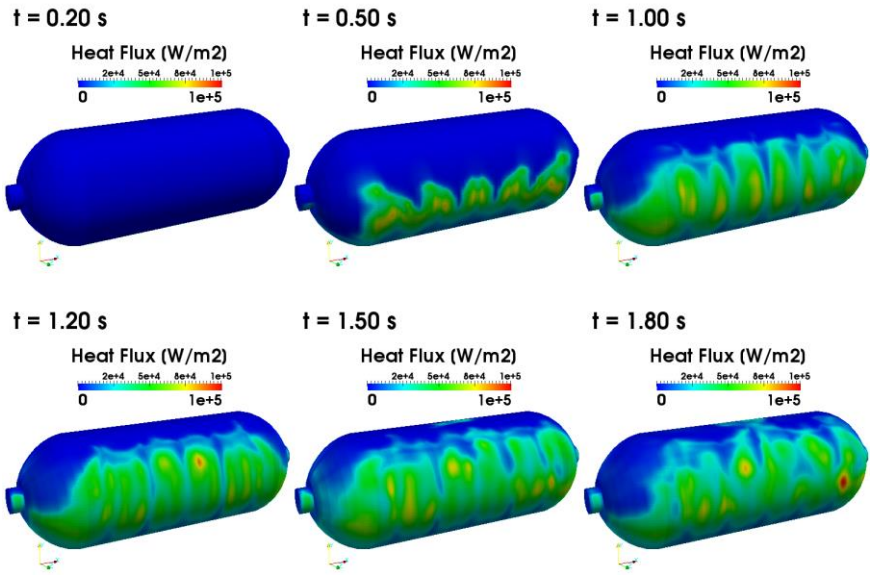

Figure 5. Cylinder wall heat flux distribution at t = 0.2, 0.5, 1.0, 1.2, 1.5, and 1.8 s.

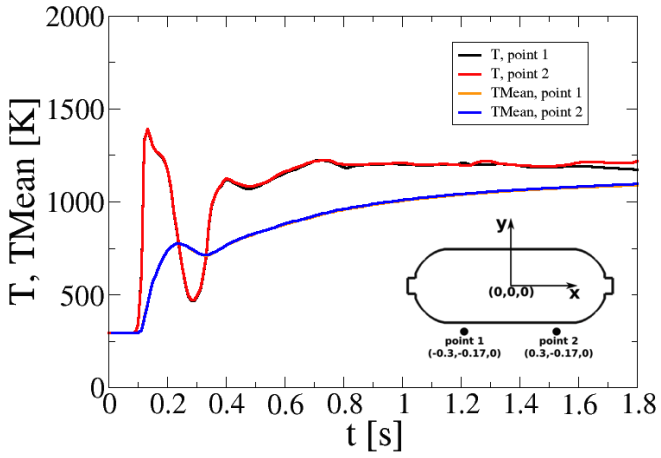

Figure 6. Time evolution of instantaneous and mean temperature at two monitoring points.

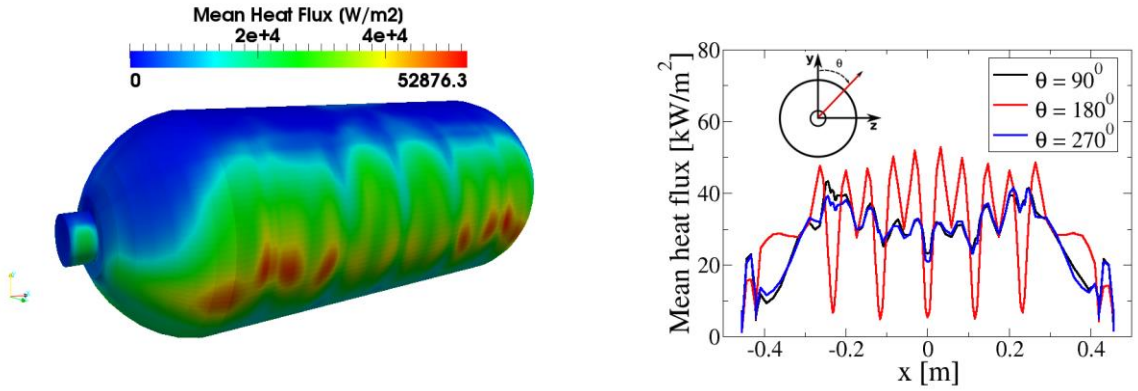

Figure 7. Mean heat flux at cylinder wall (left) and axial distributions of mean heat flux at three different angles in the y-z plane (90^0, 180^0, 270^0) (right).

The thermal simulation was carried out until final time t = 600 s. The temperature fields at t = 120, 300, and 600 s for $\theta = 90^0$ and 180^0 are shown in Figure 8. In both cases, the heat transfer rate seems to be more or less similar, as the heating proceeds towards 600 s. The maximum temperatures for both cases are also similar. However, for the 180^0 case (lower surface of the cylinder), localized heat spots are formed due to spatial fluctuation of the external heat flux as shown in Figure 7 (left). These localized heating is caused by the arrangement of propane nozzle below the cylinder.

The heating by the external propane fire also leads to the decomposition of the CFRP, as represented by the density rate of change (Equation 3). Once the decomposition temperature onset is reached, the decomposition reaction starts to consume continuously the CFRP resin. The density ratio fields, i.e. the ratio between the instantaneous CFRP density and the initial density, are shown in Figure 9. For both cases, the decomposition rate looks equal, most probably due to the same heat transfer rate. At t = 600 s, about half of the CFRP in the through-thickness direction has been completely decomposed. Again, for the 180^0 case, localized decomposition is observed at t = 120 and 300 s due to localized heat flux at the outer boundary.

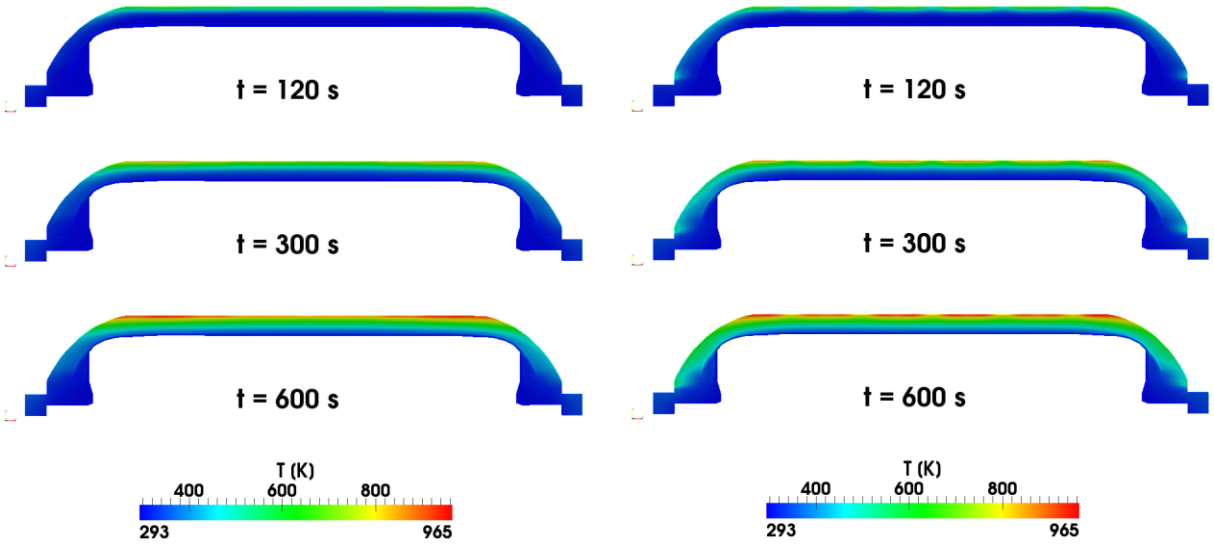

Figure 8. Temperature fields of hydrogen cylinder at t = 120, 300, 600 s for $\theta = 90^0$ (left) and 180^0 (right).

5.3 Fire Resistance

One of the practical interests in the current study is to estimate the cylinder fire resistance, i.e. how much time it takes for the cylinder to withstand the fire heating until its structure fails. At this stage, a simple criterion based on the internal pressure increase is used. As the tank is continuously heated by the fire, its internal pressure increases from initially 343 bar up to the point when the tank structure fails. In the corresponding experiment, the pressure at failure is 357 bar [3]. In this study, the fire resistance is predicted by monitoring the internal pressure and spot the time at which the failure pressure of 357 bar is reached. We predict the internal pressure increase using the following equation on internal pressure-temperature relation fitted from a fire experiment on a type-IV cylinder [12]:

$$p = 1.2T + 320 \quad (6)$$

In the above equation, p is in bar and T is in ^{0}C.

The time evolution of the tank internal pressure increase is shown in Figure 10. The failure pressure in the corresponding experiment (357 bar) is reached at 399 s (6 mins 39 seconds). This value is in a good agreement with the reported fire resistance in the corresponding experiment, i.e. 6 mins 27 seconds [3]. This agreement demonstrates that the combination between LES for fire simulation using FireFOAM and FE thermal analysis of the hydrogen cylinder used in the present study is able to predict realistically the fire dynamics and the cylinder fire resistance.

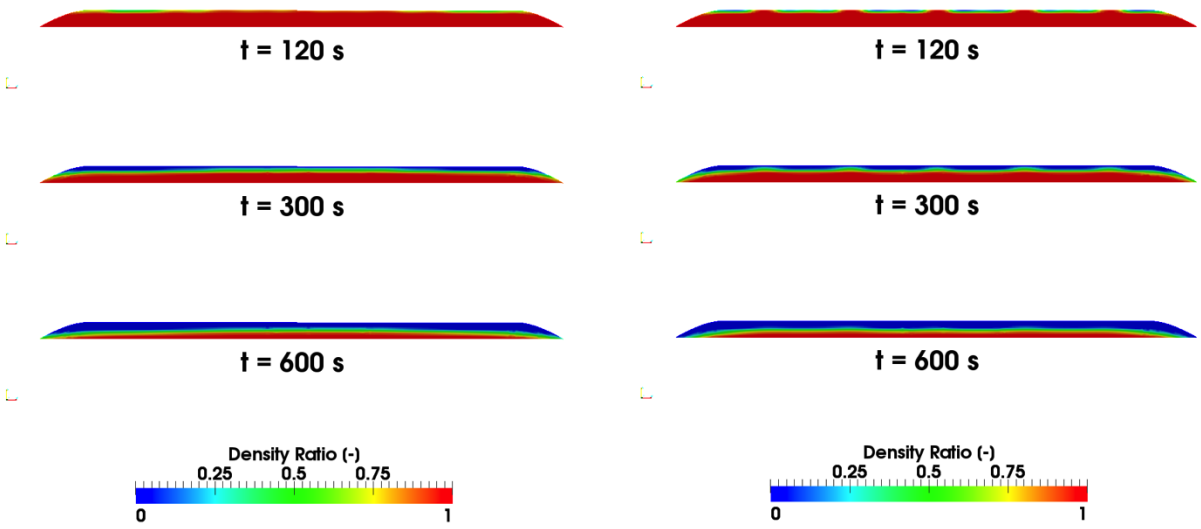

Figure 9. Density ratio fields at t = 120, 300, 600 s for θ = 90^0 (left) and 180^0 (right). Note: The figure is zoomed-in to capture only the affected area in the CFRP material (the plastic liner and metallic boss are omitted).

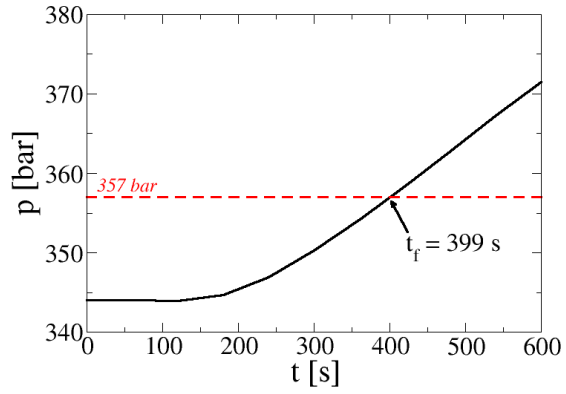

Figure 10. Time evolution of tank internal pressure.

6.0 CONCLUSION

In this paper, simulations of thermal fields of type-4 hydrogen tank cylinder subjected to external propane fires, mimicking a reported corresponding experiment [3], have been presented. The thermal response of the cylinder is modelled within a Finite Element framework, taking into account effects of thermal decomposition reaction and volatile gas transport. The model is implemented into the open source FE code Elmer. The external propane fire is predicted with the Large Eddy Simulation technique using the open source CFD code FireFOAM, in which a combustion model based on an extended Eddy Dissipation Concept is implemented. The mean heat flux distribution on the cylinder wall predicted by FireFOAM is used as a boundary condition in the Elmer simulation. It was found that around 50% of the cylinder CFRP material has been decomposed after 600 s. Using a simple failure criterion based on the internal pressure increase, it can be predicted that the cylinder fire resistance is 6 mins 39 seconds, which is in a good agreement with the reported fire resistance of 6 mins 27 seconds in the experiment. This demonstrates the potential of the combined CFD-FE simulations employed in the present study in order to predict the cylinder fire resistance. However, despite this agreement, a more comprehensive analysis covering the thermo-mechanical aspect of the cylinder is needed in the future work, so as to validate the rudimentary assumption of failure criteria used in the current analysis.

7.0 ACKNOWLEDGEMENTS

This work is carried out under the ESPRC project EP/K021109/1. The collaboration with the participating groups in the project (University of Ulster, University of Bath, and the advisory board) is gratefully acknowledged.

8.0 REFERENCES

1. Gentilhomme O., Proust C., Jamois D., Tkatschenko I., Cariteau B., Studer E., Masset F., Joncquet G., Amielh M., and Anselmet F., Data for the Evaluation of Hydrogen Risks Onboard Vehicles: Outcomes from the French Project Drive, *International Journal of Hydrogen Energy*, **37**, No. 22, 2012, pp. 17645-17654.
2. Weyandt N., Vehicle Bonfire to Induce Catastrophic Failure of a 5,000-PSIG Hydrogen Cylinder Installed on a Typical SUV, Final report – SwRI Project N° 01.06939.01.005-28, 2006.
3. Zalosh R., and Weyandt N., Hydrogen Fuel Tank Fire Exposure Burst Test, SAE paper number 2005-01-1886, 2005.
4. Brennan S., and Molkov V., Safety Assessment of Unignited Hydrogen Discharge from Onboard Storage in Garages with Low Levels of Natural Ventilation, *International Journal of Hydrogen Energy*, **38**, No. 19, 2013, pp. 8159-8166.
5. Henderson J.B., Wiebelt J.A., and Tant M.R., A Model for Thermal Response of Polymer Composite Materials with Experimental Verification, *Journal of Composite Materials*, **19**, 1985, pp. 579-595.
6. Sullivan R.M., A Coupled Solution Method for Predicting the Thermostructural Response of Decomposing, Expanding Polymeric Composites, *Journal of Composite Materials*, **27**, 1993, pp. 408-434.
7. McManus H.L., and Springer G.S., High Temperature Behaviour of Thermomechanical Behaviour of Carbon-phenolic and Carbon-carbon Composites, I. Analysis, *Journal of Composite Materials*, **26**, 1992, pp. 206-229.
8. Gibson A.G., Wu Y.S., Chandler H.W., Wilcox J.A.D., and Bettess P., A Model for the Thermal Performance of Thick Composite Laminates in Hydrocarbon Fires, *Rev. L'Inst Franc Petrol*, 1995, **50**, pp. 69-74.

9. Dimitrienko Y.I., Thermomechanical Behaviour of Composite Materials and Structures under High Temperatures: 1. Materials, *Composites*, **28A**, 1997, pp. 453-461.
10. Zheng J., Bie H., Xu P., Chen H., Liu P., Li X., and Liu Y., Experimental and Numerical Studies on Bonfire Test of High-Pressure Hydrogen Storage Vessels, *International Journal of Hydrogen Energy*, **35**, No. 15, 2010, pp. 8191-8198.
11. Ojha M., Dhiman A.K., and Guha K.C., Simulation of Thermally Protected Cylindrical Container Engulfed in Fire, *Journal of Loss Prevention in the Process Industries*, **35**, No. 2, 2012, pp. 391-399.
12. Hu J., Chen J., Sundararaman S., Chandrashekhara K., and Chernicoff W., Analysis of Composite Hydrogen Storage Cylinders Subjected to Localized Flame Impingements, *International Journal of Hydrogen Energy*, **33**, No. 11, 2008, pp. 2738-2746.
13. Zheng J., Ou K., Bie H., Xu P., Zhao Y., Liu X., and He Y., Heat Transfer Analysis of High-Pressure Hydrogen Storage Tanks Subjected to Localized Fire, *International Journal of Hydrogen Energy*, **37**, No. 17, 2012, pp. 13125-13131.
14. Zheng J., Ou K., Hua Z., Zhao Y., Xu P., Hu J., and Han B., Experimental and Numerical Investigation of Localized Fire Test for High-Pressure Hydrogen Storage Tanks, *International Journal of Hydrogen Energy*, **38**, No. 25, 2013, pp. 10963-10970.
15. Raback, P., Malinen, M., Ruokolainen, J., Pursula, A., and Zwinger, T., Elmer Models Manual, CSC-IT Center for Science, Helsinki, Finland, 2014.
16. http://code.google.com/p/firefoam-dev
17. Wang C.J., Wen J.X., Chen Z.B., and Dembele S., Predicting Radiative Characteristics of Hydrogen and Hydrogen/Methane Jet Fires using FireFOAM, *International Journal of Hydrogen Energy*, **39**, No. 35, 2014, pp. 20560-20569.
18. Chen Z.B., Wen J.X., Xu B.P., and Dembele S., Large Eddy Simulation of a Medium-Scale Methanol Pool Fire using the Extended Eddy Dissipation Concept, *International Journal of Heat and Mass Transfer*, **70**, 2014, pp. 398-408.
19. Chen Z.B., Wen J.X., Xu B.P., and Dembele S., Extension of the Eddy Dissipation Concept and Smoke Point Soot Model to the LES Frame for Fire Simulations, *Fire Safety Journal*, **64**, 2014, pp. 12-26.
20. Idemat Database, Delft University of Technology, 2003.